



# Simultaneous Capture, Detection, and Inactivation of Bacteria as Enabled by a Surface-Enhanced Raman Scattering Multifunctional Chip\*

Houyu Wang, Yanfeng Zhou, Xiangxu Jiang, Bin Sun, Ying Zhu, Hui Wang, Yuanyuan Su, and Yao He\*

**Abstract:** Herein, we present a multifunctional chip based on surface-enhanced Raman scattering (SERS) that effectively captures, discriminates, and inactivates pathogenic bacteria. The developed SERS chip is made of a silicon wafer decorated with silver nanoparticles and modified with 4-mercaptophenylboronic acid (4-MPBA). It was prepared in a straightforward manner by chemical reduction assisted by hydrogen fluoride etching, followed by the conjugation of 4-MPBA through Ag–S bonds. The dominant merits of the fabricated SERS chip include excellent reproducibility with a relative standard deviation (RSD) value smaller than 11.0 %, adaptable bacterial-capture efficiency (ca. 60 %) at low concentrations (500–2000 CFU mL<sup>−1</sup>), a low detection limit (down to a concentration of  $1.0 \times 10^2$  cells mL<sup>−1</sup>), and high antibacterial activity (an antibacterial rate of ca. 97 %). The SERS chip enabled sensitive and specific discrimination of *Escherichia coli* and *Staphylococcus aureus* from human blood.

Every year over 300 million cases of serious and even fatal diseases are caused by bacterial infections or contaminations (e.g., tuberculosis, resistant “superbug” infections) with the loss of over 2 million lives.<sup>[1]</sup> A consensus has been reached that survival rates could be greatly improved if bacterial infections could be effectively diagnosed at an early stage.<sup>[2]</sup> Therefore, the rapid, sensitive, and low-cost detection of pathogenic bacteria in clinical samples (e.g., saliva, phlegm, and blood) has been an urgent demand. The well-established clinical gold standard of bacteria culture is efficacious for the analysis of pathogens; however, this method involves complex

and time-consuming biochemical characterization procedures, including long-term culture in selective media (up to several days), morphological analysis of bacterial colonies, and immunoassays of bacterial metabolites.<sup>[3]</sup> To address this issue, strategies based on the polymerase chain reaction (PCR) and sequencing have been developed for rapid microbiological identification in assay times of several hours (ca. 6–10 h).<sup>[4]</sup> Nonetheless, these methods also involve tedious procedures to some extent (e.g., cell lysis, nucleic-acid extraction, and signal amplification), thus limiting their widespread application in point-of-care diagnosis. Furthermore, they are usually unable to distinguish bacteria with low concentrations (e.g., < 100 CFU mL<sup>−1</sup>).<sup>[5]</sup>


Scientists have developed elegant optical analytical techniques (e.g., colloidal-gold-based colorimetric sensing, assays based on fluorescent or chemically luminescent probes, and spectral analysis based on surface-enhanced Raman scattering (SERS)) for biosensing and bioanalysis.<sup>[6]</sup> In particular, recent advancements include methods for the rapid (tens of minutes to several hours) and sensitive (even down to single bacteria) detection of bacteria.<sup>[7]</sup> Among these techniques, SERS has emerged as a powerful analytical tool that enables the label-free and sensitive detection of various biological and chemical species (e.g., DNA, proteins, cells, and bacteria) owing to its three outstanding features: 1) giant Raman signal enhancement (enhancement factor (EF) values can be up to  $10^{6-9}$ ), 2) narrow and representative Raman fingerprinting spectra, which enable the multiplexed identification of targets from real samples, and 3) nondestructive data acquisition through simple manipulation without staining or specific modification.<sup>[8]</sup> Although these reported approaches have shown especially high efficacy for the discrimination of bacteria, there is increasing demand for the development of novel platforms with multiple abilities: the capture, detection, and inactivation of tiny bacteria.<sup>[2]</sup> However, no such multifunctional platform has yet been reported.

Herein, we introduce a SERS multifunctional chip made of a silicon wafer decorated with silver nanoparticles and modified with 4-mercaptophenylboronic acid (4-MPBA). The SERS chip integrates the three capabilities of bacterial capture, analysis, and sterilization. It features adaptable bacterial-capture efficiency of typically about 60 % even at low concentrations (500–2000 CFU mL<sup>−1</sup>). Meanwhile, as a result of the high antibacterial activity and excellent surface plasmonic resonance (SPR) performance of AgNPs, the SERS chip enables reproducible and sensitive bacteria detection (ca.  $1.0 \times 10^2$  cells mL<sup>−1</sup>) with robust and strong

[\*] Dr. H. Wang,<sup>[†]</sup> Dr. Y. Zhou,<sup>[†]</sup> X. Jiang,<sup>[†]</sup> B. Sun, Y. Zhu, H. Wang, Dr. Y. Su, Prof. Y. He  
Institute of Functional Nano & Soft Materials (FUNSOM) and Collaborative Innovation Center of Suzhou Nanoscience and Technology (NANO-CIC), Soochow University  
Suzhou 215123 (China)  
E-mail: yaohe@suda.edu.cn

[†] These authors contributed equally to this work.

[\*\*] We express our sincere thanks to Prof. Shuit-Tong Lee for fruitful discussions. This research was supported by the National Basic Research Program of China (973 Program 2013CB934400, 2012CB932400), the NSFC (61361160412, 31400860), and a project funded by the Priority Academic Program Development of Jiangsu Higher Education Institutions (PAPD), Jiangsu Key Laboratory for Carbon-based Functional Materials & Devices, and the China Postdoctoral Science Foundation (2014M550300).

 Supporting information for this article is available on the WWW under <http://dx.doi.org/10.1002/anie.201412294>.

antibacterial activity (an antibacterial rate of ca. 97%). We further demonstrate that this kind of high-performance chip is able to distinguish different bacteria in human blood.

To construct the SERS chip, we first modified a planar silicon wafer in situ with Ag NPs (Ag NPs@Si) through an established HF etching method.<sup>[8d,e]</sup> Next, bacteria-binding molecules of 4-MPBA were introduced onto the prepared Ag NPs@Si substrate through covalent binding through Ag–S bonds (Figure 1 A(a); a photograph of the chip ( $1.2 \times 2.8 \text{ cm}^2$ ) is also shown). The 4-MPBA molecule contains three functional groups: a thiol group for conjugation with Ag NPs, a boronic acid group that reversibly binds peptidoglycan from the cell wall of bacteria,<sup>[9]</sup> thus leading to the specific capture of various kinds of bacteria (Figure 1 A(b)), and a benzene ring that significantly amplifies SERS signals of the captured bacteria (Figure 1 A(c)). As well as sensitive bacterial detection, the resultant chip enables efficient bacterial inactivation as a result of  $\text{Ag}^+$  ions released from Ag NPs immobilized on the substrate (Figure 1 A(d)).<sup>[10]</sup> Scanning electron microscopy (SEM) and atomic force microscopy (AFM) images of Ag NPs@Si revealed that Ag NPs with an average size of approximately 110 nm were uniformly distributed on the surface of the silicon wafer (Figure 1 B). Moreover, the spacing between the superficial Ag NPs was between 50 and 150 nm, which is much smaller than the diameter of a bacterium (micrometer scale), thus guaranteeing that the captured bacteria can lie flat on the surface of the chip.<sup>[7c]</sup> For proof-of-concept experiments, we chose the representative Gram-negative bacterium *Escherichia coli* and Gram-positive bacterium *Staphylococcus aureus* as model bacteria. SEM showed that few bacteria in LB medium were nonspecifically absorbed on the pure silicon wafer (Figure 1 C(a,c)). In sharp contrast, much more bacteria were captured by 4-MPBA–Ag NPs@Si (Figure 1 C(b,d)), thus demonstrating the high specificity and efficiency of the SERS chip for bacterial capture.

Bacteria were captured by the SERS chip in a concentration- and time-dependent manner (Figure 2 A). In particular, Figure 2 A(a) suggests that the number of bacteria captured by the chip increases as the 4-MPBA concentration increases. Figure 2 A(b) displays the quantitative evaluation of the bacterial-capture yields at different capture times.

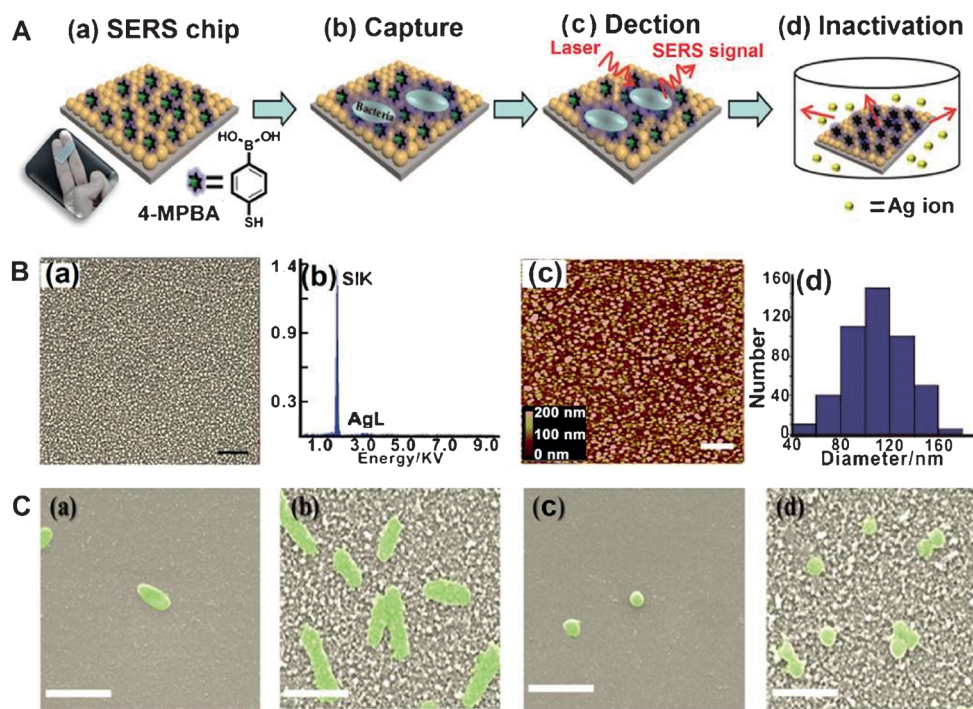


**Figure 1.** A) Schematic illustration (not drawn to scale) of a) the SERS chip and b–d) the capture, detection, and inactivation of bacteria with the multifunctional SERS chip (blue ellipses represent bacteria). A photograph of a SERS chip is also shown in (a). B) a) SEM image, b) EDX pattern, c) AFM image, and d) Ag NP size distribution of the as-prepared Ag NPs@Si substrates (scale bars: 1  $\mu\text{m}$ ). C) a,b) SEM images of *E. coli* on the pure silicon wafer (a) and the fabricated chip (b); c,d) SEM images of *S. aureus* on the pure silicon wafer (c) and the prepared chip (d; scale bars: 2  $\mu\text{m}$ ).

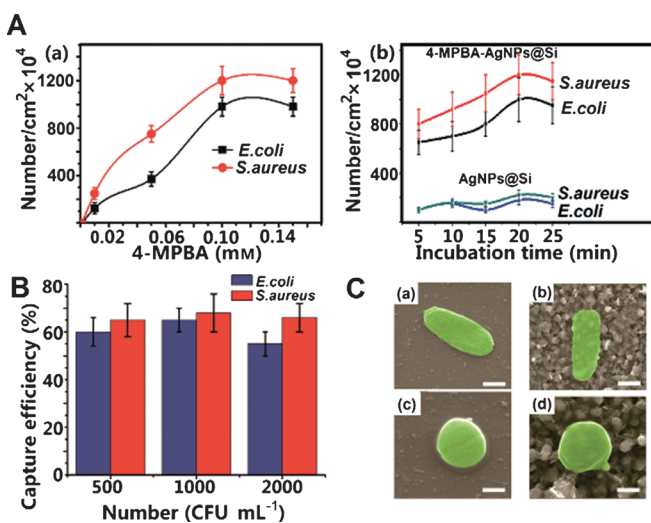


**Figure 2.** A) Graphs showing a) the number of bacteria per square centimeter on the chip at different concentrations of 4-MPBA after incubation for 20 min and b) the number of bacteria per square centimeter on the chip modified with 0.1 mM 4-MPBA and on Ag NPs@Si without 4-MPBA modification at different incubation times. The test LB media contained bacteria at a high concentration of  $4.0 \times 10^8 \text{ CFU mL}^{-1}$ . B) Bacterial-capture efficiency of the chip at low bacterial concentrations ranging from 500 to 2000  $\text{CFU mL}^{-1}$ . The capture experiments were performed with an incubation time of 20 min. All error bars show the standard deviation determined from three independent assays. C) SEM images of a single bacterium attached on a,c) a pure silicon wafer and b,d) the SERS chip (scale bars: 0.5  $\mu\text{m}$ ). *E. coli* and *S. aureus* were chosen as the model bacteria in all experiments.



Typically, when such SERS chips were immersed in LB medium containing bacteria at a high concentration of  $4.0 \times 10^7$  CFU mL<sup>-1</sup> for 20 min, maximum values were reached (ca.  $1200 \times 10^4$  and  $1000 \times 10^4$  cm<sup>2</sup> for *S. aureus* and *E. coli*, respectively) at a 0.1 mM concentration of 4-MPBA; these amounts of bacteria are five times as high as those captured by the pure Ag NPs@Si substrate without 4-MPBA modification (i.e., ca.  $250 \times 10^4$  cm<sup>2</sup> for *S. aureus* and ca.  $200 \times 10^4$  cm<sup>2</sup> for *E. coli*). Even at low bacteria concentrations ranging from 500 to 2000 CFU mL<sup>-1</sup>, the chip also showed adaptable bacterial-capture efficiency (ca. 60%) for both *E. coli* and *S. aureus* (Figure 2B), thus implying the feasibility of the capture and analysis of tiny bacteria in clinical samples (for a detailed calculation of capture efficiency, see the Supporting Information). Figure 2C shows the morphology of bacteria attached to the SERS chip and a pure silicon wafer. In contrast to the intact cell wall of *E. coli* or *S. aureus* adhered to the silicon wafer (Figure 2C(a,c)), a larger and thinner rim of *E. coli* or *S. aureus* is formed through stretching of the cell wall of bacteria captured on the chip (Figure 2C(b,d)) owing to the strong interaction between bacteria and binding molecules, in good agreement with previously reported studies.<sup>[11]</sup>

Such high-efficacy bacteria capture makes the SERS chip suitable for the efficient separation and sensitive detection of clinical bacteria. By taking advantage of the high SERS enhancement of Ag NPs@Si (enhancement factor:  $1.3 \times 10^7$ ),<sup>[8d,e]</sup> our chip yielded strong SERS intensity of 4-MPBA as high as 9000, which is in sharp contrast to the feeble Raman signals of 4-MPBA molecules ( $< 400$ ) dispersed on a pure silicon wafer under the same experimental conditions (see Figure S1 in the Supporting Information). More importantly, excellent reproducibility was observed with the chip owing to the steady immobilization of Ag NPs on the silicon support, which efficiently restricts the random movement and aggregation of free Ag NPs.<sup>[8b-c]</sup> Uniform SERS spectra of 4-MPBA recorded from 100 random spots on the substrate were obtained (Figure 3A), with a small RSD value of 10.52%, thus demonstrating the high reproducibility of the prepared SERS-active substrates. Similar SERS spectra of *E. coli* and *S. aureus* obtained from six different batches of samples were also observed (see Figure S2), thus indicating the excellent reproducibility of such SERS chips for bacteria detection. The reproducibility is superior to that of conventional SERS strategies based on the mixing of metal NPs with bacteria.<sup>[8b,c]</sup>

We further investigated the bacterial-sensing ability of our SERS chip by comparing the SERS spectra of *E. coli* and

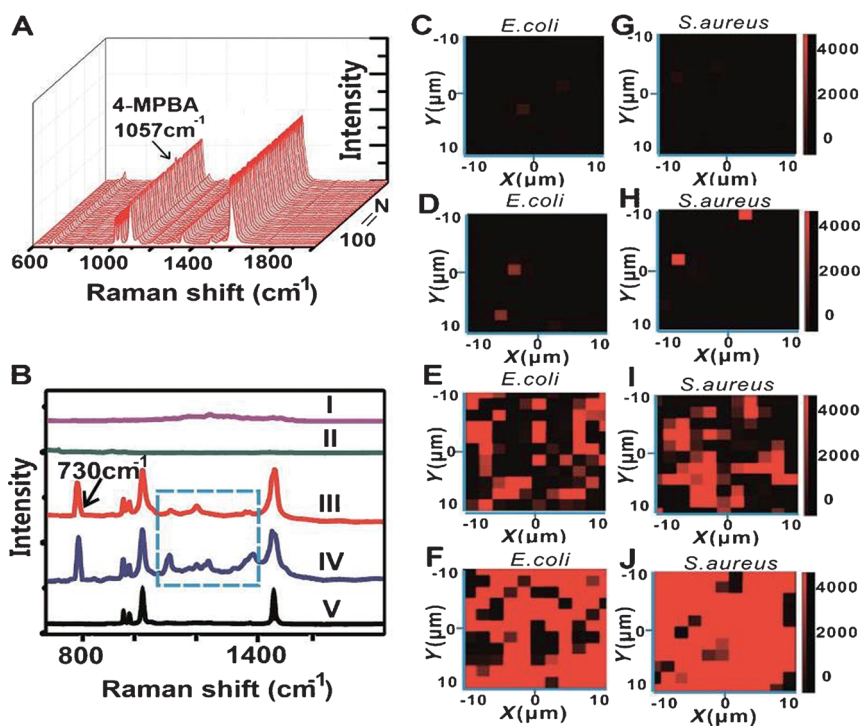


**Figure 3.** A) Raman spectra of 4-MPBA as recorded at 100 random spots on the SERS chip. B) Raman spectra of Ag NPs@Si incubated with *E. coli* (I) and *S. aureus* (II), the chip incubated with *E. coli* (III) and *S. aureus* (IV), and pure 4-MPBA-Ag NPs@Si without treatment with bacteria (V). The blue dotted box shows the bacterial fingerprint recognition bands in the range between 1128 and 1388 cm<sup>-1</sup>. The arrow indicates the distinct Raman peak at 730 cm<sup>-1</sup>. The test LB media contained *E. coli* or *S. aureus* at a concentration of  $1 \times 10^5$  cells mL<sup>-1</sup>. C–F) SERS mapping of *E. coli* on 4-MPBA-Ag NPs@Si at different concentrations of  $1 \times 10^2$  (C),  $1 \times 10^3$  (D),  $1 \times 10^5$  (E), and  $1 \times 10^7$  cells mL<sup>-1</sup> (F). G–J) SERS mapping of *S. aureus* on the chip at different concentrations of  $1 \times 10^2$  (G),  $1 \times 10^3$  (H),  $1 \times 10^5$  (I), and  $1 \times 10^7$  cells mL<sup>-1</sup> (J). Parameters for the SERS experiments:  $\lambda_{\text{ex}} = 633$  nm, acquisition time: 1 s, confocal hole: 200  $\mu\text{m}$ , slit: 100  $\mu\text{m}$ , grating: 600 g mm<sup>-1</sup>.

*S. aureus* (Figure 3B). The Raman spectra of pure 4-MPBA-Ag NPs@Si without incubation with bacteria and Ag NPs@Si incubated with *E. coli* or *S. aureus* bacteria were used as controls. Typically, in contrast to the very low intensities of the Raman signals observed in the control group of bacteria-treated Ag NPs@Si (Figure 3B, I,II), strong SERS signals were observed for the 4-MPBA-Ag NPs@Si with captured bacteria (Figure 3B, III,IV), thus suggesting that the 4-MPBA molecules greatly facilitate enhancement of the Raman signals of bacteria. As mentioned above, the bacterial cell wall is pulled by the binding 4-MPBA molecules toward the Ag NPs@Si substrate (Figure 2C(b,d)); in this way, the gaps between the Ag NPs are filled. The gaps are considered to be the “hot junctions” for the electromagnetic enhancement of Raman scattering; therefore giant SERS signals are observed for the bacteria.<sup>[11a,12]</sup> Moreover, although there are three sharp peaks (i.e., at 1000, 1024, and 1057 cm<sup>-1</sup>) below 1100 cm<sup>-1</sup> and one sharp peak at 1587 cm<sup>-1</sup> in the SERS spectrum of 4-MPBA (see Figure 3B, V), these typical Raman bands of 4-MPBA do not interfere with representative bacterial fingerprint bands in the range between 1128 and 1388 cm<sup>-1</sup> (see the blue dotted box in Figure 3B) or the distinct Raman peak at 730 cm<sup>-1</sup> (assigned to the glucosidic

bond of the bacterial cell wall; see Table S1) observed in both the *E. coli* and *S. aureus* groups.

Distinct differences in the SERS spectra of *E. coli* and *S. aureus* are found in the fingerprint recognition bands from approximately 1128 to 1388  $\text{cm}^{-1}$ . Specifically, sharp Raman peaks at about 1128 (amide III), 1240 ( $\delta(\text{CH}_2)$  amide III), and 1388  $\text{cm}^{-1}$  ( $\nu(\text{COO}^-)$  and  $\delta(\text{C-H})$  proteins) were observed in the SERS spectrum of *S. aureus*. For the *E. coli* group, an SERS spectrum with a lower magnitude was detected, as a result of the difference in the biochemical constituents of the microorganisms.<sup>[13]</sup> Moreover, one relatively sharp Raman peak at about 1280  $\text{cm}^{-1}$  ( $\delta(\text{CH}_2)$  amide III) appeared in the SERS spectrum of *S. aureus* but was not detectable in that of *E. coli*. These spectral results imply that our SERS chip features good capability for discriminating different kinds of bacteria. The performance of the chip in the detection of bacteria at different concentrations was further evaluated by SERS mapping of a selected area of  $20 \times 20 \mu\text{m}^2$  with a  $2 \mu\text{m}$  step size. The change in the Raman intensity of the peak at  $730 \text{ cm}^{-1}$  peak was recorded to quantify the *E. coli* and *S. aureus* concentrations. The red points in the SERS mapping results correspond to the SERS signals of bacteria, and the number of red points increased as the bacterial concentration increased (Figure 3C–J). The relationship between the number of red points and the actual logarithmic bacterial concentration (see Figure S3) suggests that the low limit of detection (LOD) of the SERS chip for bacteria detection ( $1.0 \times 10^2 \text{ cells mL}^{-1}$ ) lies within a large dynamic detection range (up to  $1 \times 10^7 \text{ cells mL}^{-1}$ ).

As a real application of the SERS chip, we tested human blood samples spiked with bacteria. Blood cells with sizes of approximately  $5 \mu\text{m}$  could be readily identified by optical microscopy (Figure 4A,B), whereas smaller-sized bacteria (ca.  $0.5 \mu\text{m}$ ) added to blood could not be observed at the same resolution. However, distinct SERS spectra were observed for both *E. coli* and *S. aureus* with clear fingerprint recognition bands at 1128–1388  $\text{cm}^{-1}$  (Figure 4C), identical to those of bacteria captured from LB medium (see Figure 3B). In contrast, in the Raman spectrum of the pure blood sample (blue line), a smooth line without detectable Raman peaks was observed in the range of 1100–1400  $\text{cm}^{-1}$ , thus suggesting that blood cells had little influence on the bacterial-sensing results. Significantly, the concentration of *E. coli* or *S. aureus* in human blood could be readily identified down to about  $1.0 \times 10^2 \text{ cells mL}^{-1}$  by the SERS chip, thus indicating that the developed SERS chip is sensitive enough to detect bacteria in the blood of patients suffering from blood-stream infections (e.g., ca.  $100 \text{ cells mL}^{-1}$ ).<sup>[2b]</sup> These data suggest good feasibility of the presented SERS chip for bacterial detection in real systems.

In the following experiment, the antibacterial ability of the constructed SERS chip was evaluated on the basis of the measurement of microbial viability. *E. coli* or *S. aureus* growth medium treated with a pure silicon wafer was turbid after incubation for 24 h because of rapid microbial proliferation (Figure 5A). In marked contrast, the media incubated with 4-MPBA–Ag NPs@Si for 24 h still remained pellucid, thus suggesting high antibacterial activity of the chip. The bacterial media cultured for 24 h (shown in Figure 5A) was

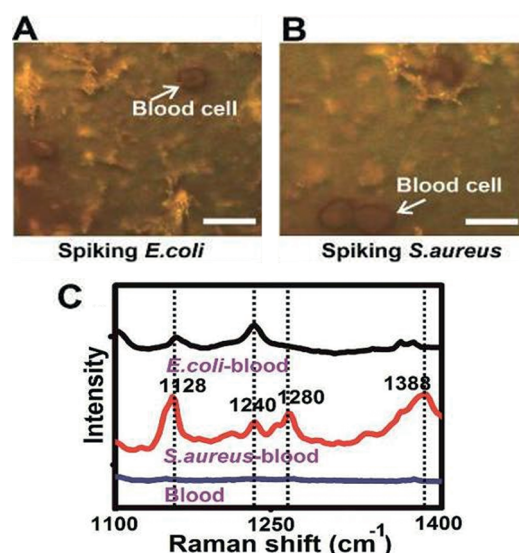


**Figure 4.** A,B) Optical microscopy images of 4-MPBA–Ag NPs@Si incubated with human blood samples containing *E. coli* (A) and *S. aureus* (B) at a concentration of  $1 \times 10^5 \text{ cells mL}^{-1}$  (scale bars:  $10 \mu\text{m}$ ). C) SERS spectra of human blood spiked with *E. coli* or *S. aureus* in the range from 1100 to 1400  $\text{cm}^{-1}$ . Human blood without bacteria was used as the control. Parameters for the SERS experiments:  $\lambda_{\text{ex}} = 633 \text{ nm}$ , acquisition time: 1 s, confocal hole:  $200 \mu\text{m}$ , slit:  $100 \mu\text{m}$ , grating:  $600 \text{ g mm}^{-1}$ .

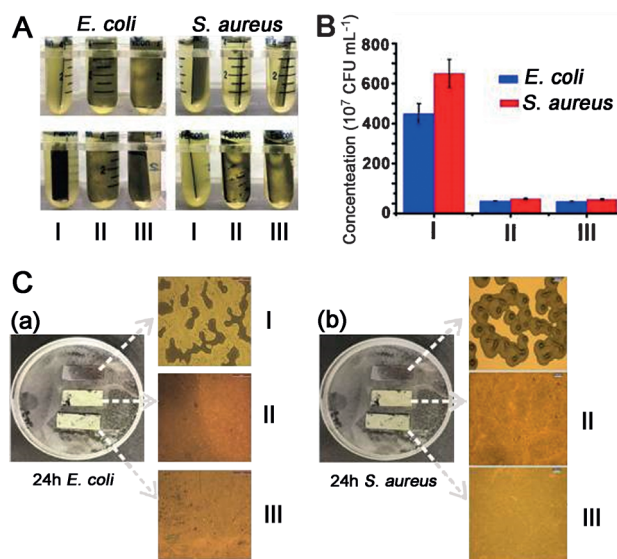


**Figure 5.** A) Antibacterial activities of silicon wafers (I), Ag NPs@Si (II), and the SERS chip (III) toward *E. coli* and *S. aureus* as determined by turbidity assays in LB medium. B) Quantitative analysis of the antibacterial ability of these three kinds of substrates by use of the standard colony-counting method. The antibacterial tests were performed by the incubation of substrates with bacterial growth media for 24 h. The error bars show the standard deviation determined from three independent assays. C) Evaluation of the antibacterial activity of the surfaces of the three kinds of substrates. a,b) Enlarged micrographs are shown of *E. coli* (a) and *S. aureus* (b) grown on the three kinds of substrates.

diluted  $1 \times 10^5$  times, then spread uniformly onto agar plates and incubated at  $37^\circ\text{C}$  for 48 h. Typically, a large number of bacterial colonies of both *E. coli* (ca. 450) and *S. aureus* (ca.

650) were observed on the agar plate in the silicon-wafer-treated groups, whereas sporadic bacterial colonies (ca. 15) emerged in the groups treated with Ag NPs@Si or 4-MPBA–Ag NPs@Si (Figure 5B). Accordingly, the antibacterial rate of our chip for *E. coli* or *S. aureus* was calculated to be as high as 97.8 or 96.9%, respectively (for the detailed calculation of the antibacterial rate, see the Supporting Information). Furthermore, the SERS chip exhibited robust and prolonged antibacterial activity; low OD<sub>600</sub> values (optical density of the medium at 600 nm) were maintained during treatment for 24 h (see Figure S4). We further employed the SERS chip to prohibit the proliferation of bacteria in solid media. Figure 5C shows enlarged images of bacterial colonies on the surfaces of different substrates. Specifically, several bacterial colonies were observed on the surface of a silicon wafer (Figure 5C, I), whereas no bacterial colony appeared on the surface of Ag NPs@Si or 4-MPBA–Ag NPs@Si (Figure 5C, II and III), thus providing further evidence of the excellent antibacterial activity of our SERS chip in solid media.

In conclusion, we have presented a type of multifunctional SERS chip with high efficacy for simultaneously capturing, sensing, and inactivating bacteria. Significantly, the fabricated chip features excellent reproducibility (RSD < 11.0%), good bacterial-capture efficiency (ca. 60%) even at low concentrations (500–2000 CFU mL<sup>-1</sup>), high sensitivity (ca. 1.0 × 10<sup>2</sup> cells mL<sup>-1</sup>), and a high antibacterial rate (ca. 97%). The SERS chip was further proven to be highly effective in capturing and discriminating bacteria in human blood, with negligible interference of blood cells in real systems. Given that this class of SERS chip can be fabricated in a facile and low-cost manner, we envision that such chips will be useful for widespread practical applications. Our findings suggest promising opportunities for the development of high-efficacy multifunctional platforms for the simultaneous detection and inactivation of pathogenic bacteria in clinical or environmental samples.

**Keywords:** bacteria · multifunctional platforms · silicon · silver nanoparticles · surface-enhanced Raman scattering

**How to cite:** *Angew. Chem. Int. Ed.* **2015**, *54*, 5132–5136  
*Angew. Chem.* **2015**, *127*, 5221–5225

- [1] a) M. E. Brecher, S. N. Hay, *Clin. Microbiol. Rev.* **2005**, *18*, 195–204; b) P. R. Shorten, A. B. Pleasants, T. K. Soboleva, *Int. J. Food Microbiol.* **2006**, *108*, 369–375; c) T. E. Ford, R. R. Colwell, *A Global Decline in Microbiological Safety of Water: A Call for Action*, American Academy of Microbiology, Washington, DC, **1996**, pp. 1–40.
- [2] a) D. C. Angus, T. van der Poll, *N. Engl. J. Med.* **2013**, *369*, 840–851; b) J. Q. Boedicker, L. Li, T. R. Kline, R. F. Ismagilov, *Lab Chip* **2008**, *8*, 1265–1272; c) A. Lee, S. Mirrett, L. B. Reller, M. P. Weinstein, *J. Clin. Microbiol.* **2007**, *45*, 3546–3548.
- [3] a) H. Y. Chu, Y. W. Huang, Y. P. Zhao, *Appl. Spectrosc.* **2008**, *62*, 922–931; b) B. S. Reisner, G. L. Woods, *J. Clin. Microbiol.* **1999**, *37*, 2024–2026.
- [4] a) A. Pechorsky, Y. Nitzan, T. Lazarovitch, *J. Microbiol. Methods* **2009**, *78*, 325–330; b) E. A. Ottesen, J. W. Hong, S. R. Quake, J. R. Leadbetter, *Science* **2006**, *314*, 1464–1467; c) J. D. Wang, X. H. Wang, Y. Li, S. D. Yan, Q. Q. Zhou, B. Gao, J. C. Peng, J. Du, Q. X. Fu, S. Z. Jia, J. K. Zhang, L. S. Zhan, *Anal. Sci.* **2012**, *28*, 237–241.
- [5] a) A. Niemz, T. M. Ferguson, D. S. Boyle, *Trends Biotechnol.* **2011**, *29*, 240–250; b) D. K. Kang, M. M. Ali, K. Zhang, S. S. Huang, E. Peterson, M. A. Digman, E. Gratton, W. Zhao, *Nat. Commun.* **2014**, *5*, 5427.
- [6] a) P. D. Howes, R. Chandrawati, M. M. Stevens, *Science* **2014**, *346*, 1247390; b) Y. W. C. Cao, R. C. Jin, C. A. Mirkin, *Science* **2002**, *297*, 1536–1540; c) Y. L. Zhong, F. Peng, X. P. Wei, Y. F. Zhou, J. Wang, X. X. Jiang, Y. Y. Su, S. Su, S. T. Lee, Y. He, *Angew. Chem. Int. Ed.* **2012**, *51*, 8485–8489; *Angew. Chem.* **2012**, *124*, 8613–8617; d) Y. L. Zhong, F. Peng, F. Bao, S. Y. Wang, X. Y. Ji, L. Yang, Y. Y. Su, S. T. Lee, Y. He, *J. Am. Chem. Soc.* **2013**, *135*, 8350–8356.
- [7] a) H. J. Chung, C. M. Castro, H. Im, H. Lee, R. Weissleder, *Nat. Nanotechnol.* **2013**, *8*, 369–375; b) W. Chen, Q. Li, W. Zheng, F. Hu, G. Zhang, Z. Wang, D. Zhang, X. Jiang, *Angew. Chem. Int. Ed.* **2014**, *53*, 13734–13739; *Angew. Chem.* **2014**, *126*, 13954–13959; c) Y. Q. Li, B. Zhu, Y. Li, W. R. Leow, R. Goh, B. Ma, E. Fong, M. Tang, X. Chen, *Angew. Chem. Int. Ed.* **2014**, *53*, 5837–5841; *Angew. Chem.* **2014**, *126*, 5947–5951; d) M. S. Mannoor, H. Tao, J. D. Clayton, A. Sengupta, D. L. Kaplan, R. R. Naik, N. Verma, F. G. Omenetto, M. C. McAlpine, *Nat. Commun.* **2012**, *3*, 763; e) J. R. Carey, K. S. Suslick, K. I. Hultkower, J. A. Imlay, K. R. C. Imlay, C. K. Ingison, J. B. Ponder, A. Sen, A. E. Wittrig, *J. Am. Chem. Soc.* **2011**, *133*, 7571–7576; f) I. Irwansyah, Y. Q. Li, W. Shi, D. Qi, W. R. Leow, M. B. Y. Tang, S. Li, X. Chen, *Adv. Mater.* **2015**, *27*, 648–654.
- [8] a) S. Schlucker, *Angew. Chem. Int. Ed.* **2014**, *53*, 4756–4795; *Angew. Chem.* **2014**, *126*, 4852–4894; b) F. Peng, Y. Y. Su, Y. L. Zhong, C. H. Fan, S. T. Lee, Y. He, *Acc. Chem. Res.* **2014**, *47*, 612–623; c) H. Wang, X. Jiang, S. T. Lee, Y. He, *Small* **2014**, *10*, 4455–4468; d) H. Wang, X. X. Jiang, X. Wang, X. P. Wei, Y. Zhu, B. Sun, Y. Y. Su, S. D. He, Y. He, *Anal. Chem.* **2014**, *86*, 7368–7376; e) X. X. Jiang, Z. Y. Jiang, T. T. Xu, S. Su, Y. L. Zhong, F. Peng, Y. Y. Su, Y. He, *Anal. Chem.* **2013**, *85*, 2809–2816; f) S. Stöckel, S. Meisel, M. Elschner, P. Rösch, J. Popp, *Angew. Chem. Int. Ed.* **2012**, *51*, 5339–5342; *Angew. Chem.* **2012**, *124*, 5433–5436.
- [9] a) L. Dzhekieva, I. Kumar, R. F. Pratt, *Biochemistry* **2012**, *51*, 2804–2811; b) S. Saito, T. L. Massie, T. Maeda, H. Nakazumi, C. L. Colyer, *Anal. Chem.* **2012**, *84*, 2452–2458.
- [10] a) S. Chernousova, M. Eppler, *Angew. Chem. Int. Ed.* **2013**, *52*, 1636–1653; *Angew. Chem.* **2013**, *125*, 1678–1696; b) C. N. Lok, C. M. Ho, R. Chen, Q. Y. He, W. Y. Yu, H. Sun, P. K. Tam, J. F. Chiu, C. M. Che, *J. Biol. Inorg. Chem.* **2007**, *12*, 527–534.
- [11] a) T. Y. Liu, K. T. Tsai, H. H. Wang, Y. Chen, Y. H. Chen, Y. C. Chao, H. H. Chang, C. H. Lin, J. K. Wang, Y. L. Wang, *Nat. Commun.* **2011**, *2*, 538; b) S. Jusuf, P. J. Loll, P. H. Axelsen, *J. Am. Chem. Soc.* **2003**, *125*, 3988–3994; c) Z. Yang, E. R. Vorpagel, J. Laskin, *J. Am. Chem. Soc.* **2008**, *130*, 13013–13022.
- [12] B. Y. Lin, C. H. Teng, H. C. Chang, J. K. Wang, Y. L. Wang, *Opt. Express* **2009**, *17*, 14211–14228.
- [13] a) K. Taylor, N. Cheng, R. Williams, A. Steven, R. Wickner, *Science* **1999**, *283*, 1339; b) H. Vogel, F. J. Jahng, *Mol. Biol.* **1986**, *190*, 191–199.

Received: December 22, 2014

Revised: February 28, 2015

Published online: March 26, 2015